Analysis of Freeze-Thaw Embolism in Conifers. The Interaction between Cavitation Pressure and Tracheid Size[1]

Jarmila Pittermann[2]* and John S. Sperry[3]

Department of Biology, University of Utah, Salt Lake City, Utah 84112

Ice formation in the xylem sap produces air bubbles that under negative xylem pressures may expand and cause embolism in the xylem conduits. We used the centrifuge method to evaluate the relationship between freeze-thaw embolism and conduit diameter across a range of xylem pressures (P_x) in the conifers *Pinus contorta* and *Juniperus scopulorum*. Vulnerability curves showing loss of conductivity (embolism) with P_x down to −8 MPa were generated with versus without superimposing a freeze-thaw treatment. In both species, the freeze-thaw plus water-stress treatment caused more embolism than water stress alone. We estimated the critical conduit diameter (D_f) above which a tracheid will embolize due to freezing and thawing and found that it decreased from 35 μm at a P_x of −0.5 MPa to 6 μm at −8 MPa. Further analysis showed that the proportionality between diameter of the air bubble nucleating the cavitation and the diameter of the conduit (kL) declined with increasingly negative P_x. This suggests that the bubbles causing cavitation are smaller in proportion to tracheid diameter in narrow tracheids than in wider ones. A possible reason for this is that the rate of dissolving increases with bubble pressure, which is inversely proportional to bubble diameter (La Place's law). Hence, smaller bubbles shrink faster than bigger ones. Last, we used the empirical relationship between P_x and D_f to model the freeze-thaw response in conifer species.

Plants living in high latitude or high altitude environments are often subject to freeze-thaw cycles during the winter season. These temperature changes present a unique challenge to the plants' xylem because ice formation in the sap leads to the creation of air bubbles in the xylem conduits. Under certain conditions, these bubbles nucleate cavitation, leading to a gas-filled (embolized) conduit that impedes water transport (Scholander et al., 1961; Hammel, 1967; Sucoff, 1969; Zimmermann, 1983).

A species' vulnerability to freezing-induced embolism rises with increasing conduit diameter (Sperry and Sullivan, 1992; Sperry et al., 1994; Davis et al., 1999; Cavender-Bares and Holbrook, 2001; Feild and Brodribb, 2001; Sperry and Robson, 2001; Pittermann and Sperry, 2003; Cavender-Bares, 2005). It is possible to estimate a critical threshold diameter above which a conduit will embolize due to freezing and thawing from experiments where the liquid-phase xylem pressure is controlled (Davis et al., 1999; Pittermann and Sperry, 2003). Thus far, the effect of xylem pressure on critical conduit diameters (D_f) for freeze-thaw embolism has only been examined at the modest pressure of −0.5 MPa (Davis et al., 1999; Pittermann and Sperry, 2003). However, plants experience a range of xylem pressures (P_x) varying from approximately −1 to −4 MPa during the winter season (Sperry and Sullivan, 1992; Sperry et al., 1994; Sparks and Black, 2000; Sparks et al., 2001; Mayr et al., 2002). We know from theory and observation that more negative P_x increases the likelihood of freezing-induced embolism (Sperry and Sullivan, 1992; Langan et al., 1997; Davis et al., 1999; Sperry and Robson, 2001), but how does variation in P_x influence the D_f for embolism? Are there other aspects of tracheid dimensions that affect the freeze-thaw embolism response? We evaluated these questions by analyzing the relationship between tracheid diameter, freeze-thaw embolism, and P_x in two species of conifers, *Juniperus scopulorum* Sarg. and *Pinus contorta* Dougl. ex Loudon.

Earlier freeze-thaw experiments performed at a liquid phase P_x of −0.5 MPa identified a threshold cavitation diameter (D_f) of approximately 44 μm. Conduits whose lumen diameter is equal to or greater than this diameter were predicted to embolize by freezing and thawing at this pressure. Interestingly, although these experiments tested stems of 12 vessel-bearing angiosperms as well as roots and stems belonging to seven tracheid-bearing gymnosperms, both angiosperm and

[1] This work was supported in part by the National Science Foundation (Dissertation Improvement Grant 0308862 to J.P. and NSF–IBN–0416297 to J.S.S.). J.P. gratefully acknowledges the support of the National Science and Engineering Research Council of Canada.

[2] Present address: Department of Integrative Biology, University of California, 4007 Valley Life Sciences Bldg., Berkeley, CA 94720.

[3] Present address: Department of Biology, University of Utah, Salt Lake City, UT 84112.

* Corresponding author; e-mail pittermann@berkeley.edu; fax 510–643–6264.

The author responsible for distribution of materials integral to the findings presented in this article in accordance with the policy described in the Instructions for Authors (www.plantphysiol.org) is: Jarmila Pittermann (pittermann@berkeley.edu).

Article, publication date, and citation information can be found at www.plantphysiol.org/cgi/doi/10.1104/pp.105.067900.

gymnosperm data converged upon a D_f value of 43 to 44 μm (Davis et al., 1999; Pittermann and Sperry, 2003). This is currently the strongest evidence we have that conduit diameter is the crucial dimension rather than conduit volume, because vessels and tracheids of the same mean diameter show the same freeze-thaw response despite tracheids being only a fraction of the length of vessels.

The dependence of freeze-thaw embolism on conduit diameter rather than volume is consistent with the pattern of freezing. The freezing of xylem sap is thought to occur centripetally, moving inward from the conduit walls (the site of ice nucleation; Robson et al., 1988; Sperry and Robson, 2001). By forcing air out of the ice crystal lattice, freezing produces centrally located bubbles, whose volume should be proportional to the cylindrical volume of freezing water from which the air came (Sperry and Sullivan, 1992; Fig. 1). This cylindrical volume will be a function of the conduit diameter and the distance (L) between bubbles in the frozen conduit. If L is constant or increases with conduit diameter, wider conduits should produce larger bubbles when frozen. Corroborating this idea are observations of frozen xylem that show that narrow conduits contain smaller air bubbles than wider conduits (Ewers, 1985). The fact that tracheids and vessels of the same diameter are equally vulnerable to freezing-induced embolism suggests that L is at the longest equal to the length of a tracheid and certainly shorter than a vessel (Fig. 1). This observation also implies that as long as the bubbles do not migrate extensively along the whole length of the conduit and coalesce during the thaw, their size will be related to conduit diameter rather than the entire conduit length and volume. Otherwise, vessels—being longer than tracheids—would be much more vulnerable for a given diameter than tracheids. However, it is unclear how altering the P_x at freezing might influence the diameter dependence of vulnerability to embolism. More negative P_x should be able to expand smaller bubbles formed in narrower tracheids. Can we predict the freeze-thaw cavitation pressure in conifer tracheids from diameter alone?

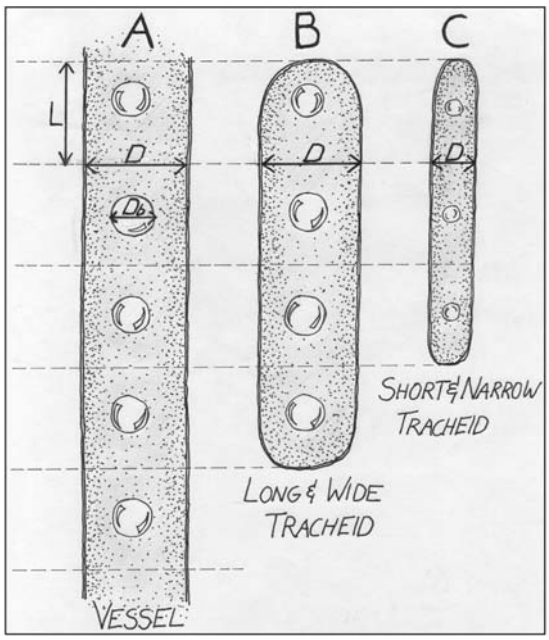

Figure 1. A simple geometric model for the relationship between bubble size and conduit size. A freezing conduit of diameter D produces centrally located air bubbles with a volume proportional to the volume of a conduit section of length L (the volume proportionality constant is the k in Eq. 2). Tracheids and vessels of similar D (vessel A and tracheid B) have been found to have similar vulnerability to cavitation by freezing and thawing, suggesting similar bubble diameter (D_b; Pittermann and Sperry, 2003). This means that L is similar for the same D and shorter than a tracheid. Species with narrower conduits (e.g. tracheid C) are more resistant to cavitation by freezing and thawing, indicating a link between bubble and conduit diameter. The conduit length per bubble (L) apparently does not increase markedly in narrower conduits; instead, L may be independent of conduit diameter (as shown) or perhaps more likely to decline with smaller D.

A theoretical scaling between tracheid size and the freeze-thaw cavitation pressure (P_x*) begins with La Place's law as applied to an air bubble in water:

$$P_x^* < -4T/D_b, \quad (1)$$

where T is the surface tension of water (0.0728 Pa m) and D_b is the diameter of an air bubble in the tracheid after thawing. The xylem pressure acting to expand the bubble (P_x*) must exceed the internal pressure exerted by surface tension ($4T/D_b$) that acts to collapse the bubble (Yang and Tyree, 1992). We can express the D_b of a spherical bubble in terms of the cylindrical water volume it came from if we assume proportionality between the bubble and water volume:

$$D_b = 1.14(kL)^{1/3}D^{2/3}, \quad (2)$$

where k is the proportionality between air bubble and water volume (bubble volume = $k \times$ cylinder water volume), D is the diameter of the cylindrical conduit, and L is the conduit length per bubble (Fig. 1). By substituting Equation 2 into Equation 1, we have a relationship between P_x* and the threshold freeze-thaw cavitation diameter (D_f):

$$P_x^* = -3.51T(kL)^{-1/3}D_f^{-2/3}. \quad (3)$$

While the D_f in this equation can be estimated from the amount of embolism (Davis et al., 1999), the kL term is unknown. Although k could be calculated from the solubility of air, this does not account for the partial dissolving of air back into the thawing sap before pressures become fully negative after the sap has sufficiently liquefied. This bubble shrinkage is potentially rapid and very critical for determining the final bubble size at cavitation (Sucoff, 1969).

From previous work (Davis et al., 1999; Pittermann and Sperry, 2003) where D_f was 44 μm at a P_x of -0.5 MPa, the kL term was 6.9×10^{-5} μm. Does this value hold across all xylem pressures? Theory gives little insight, but if kL is constant, then P_x* should scale

with $D_f^{-2/3}$. Alternatively, if k is constant but L is proportional to D_f, then P_x* should be proportional to D_f^{-1}. It is possible that k could also vary with D_f if bubbles of different sizes shrink at different rates during the thaw. A central objective of this article is to resolve the value of this proportionality and whether it is constant across a range of P_x*. If the relationship between P_x* and D_f is similar across species of conifers, we may be able to predict the vulnerability of conifers to freeze-thaw embolism from their diameter distributions. Our approach utilized the combination of centrifugal force and a controlled temperature regime (Alder et al., 1997; Davis et al., 1999; Pittermann and Sperry, 2003) to subject stem segments to a wide range of P_x during the freeze-thaw cycle.

To evaluate the effect of significant water stress on freezing-induced embolism, it was necessary to distinguish between embolism caused by the water stress alone versus any additional embolism caused by the freeze-thaw treatment. This complication was avoided in earlier work because the embolism caused by −0.5 MPa of water stress in the absence of freezing and thawing was minimal (Davis et al., 1999; Pittermann and Sperry, 2003). In this study, we used much more negative P_x and could not ignore the embolism caused by water stress alone. To account for the embolism caused specifically by the freeze-thaw treatment, we compared the water-stress vulnerability curve (no freeze-thaw) with the freeze-thaw + water-stress vulnerability curves (subjected to freezing and thawing) for the same stems. Vulnerability curves track the loss of conductivity with increasingly negative xylem pressures (Pockman et al., 1995; Alder et al., 1997). We present these data together with a reanalysis of the results of Pittermann and Sperry (2003) that for the sake of consistency account for the (usually minor) embolism caused by the modest P_x of −0.5 MPa in these experiments.

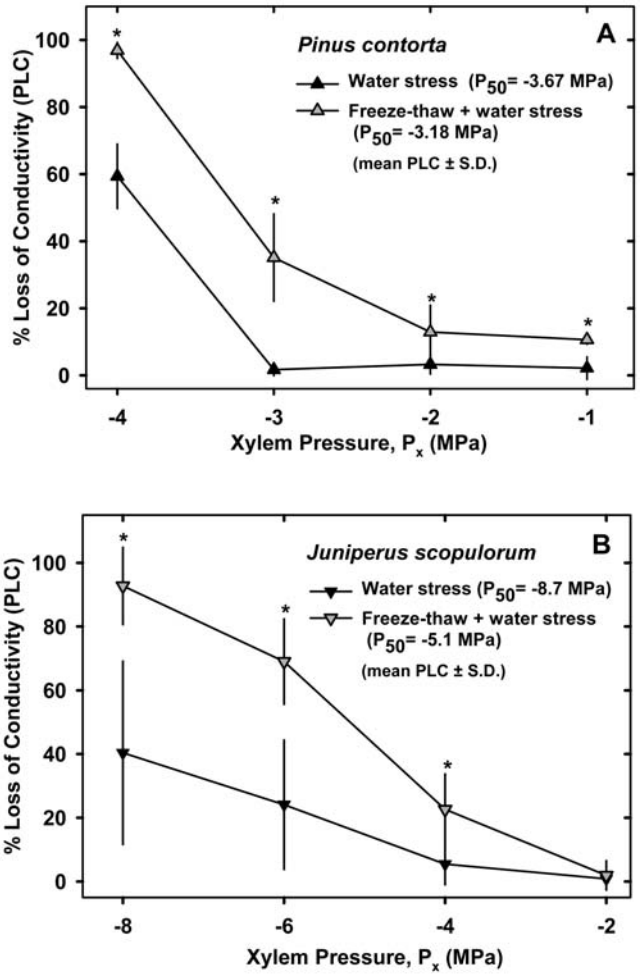

Figure 2. The water-stress and freeze-thaw + water-stress vulnerability curves of *P. contorta* (A) and *J. scopulorum* (B). Asterisks denote significantly different means for the same pressure (n = 5–6 at each P_x; mean ± SD; Student's t test, P = 0.05).

RESULTS

Vulnerability Curves and Tracheid Anatomy

Stems of both *P. contorta* and *J. scopulorum* were more vulnerable to the freeze-thaw + water-stress treatment than to water stress alone (Fig. 2, compare water-stress and freeze-thaw + water-stress vulnerability curves). In *P. contorta*, the P_x causing a 50% loss of conductivity (P_{50}, determined from a Weibull function curve fit) increased from −3.67 MPa for the water-stress curve to −3.18 MPa with the added freeze-thaw treatment. A P_x of −4 MPa combined with freezing and thawing caused a 98% loss of conductivity (PLC) versus only a 60 PLC in the absence of a freeze. In the more embolism-resistant *J. scopulorum*, the P_{50} increased from −8.7 MPa for water stress alone to −5.1 MPa for water-stress + the freeze-thaw treatment. A P_x of −8.0 MPa in combination with freezing caused approximately 94 PLC due to freezing and thawing (PLC_{FT}) versus only about 40 PLC in the absence of the freezing treatment.

The generally greater susceptibility of *P. contorta* stems to both types of embolism was consistent with their having significantly larger diameter tracheids (Student's t test, $P < 0.0001$; mean diameter ± SD; 11.02 ± 1.1 μm) than in *J. scopulorum* stems (8.44 ± 0.54 μm; Fig. 3). Furthermore, *P. contorta* also exhibited a broader range of tracheid diameters, with the largest tracheids exceeding 30 μm in diameter. By comparison, the largest tracheids in *J. scopulorum* measured approximately 20 μm.

D_f and Proportionality Coefficients (kL)

The mean critical cavitation diameter declined with increasingly negative P_x from an average of 35 μm at a P_x of −0.5 to 6 μm at a P_x of −8 MPa (Fig. 4). Scaling across all species and pressures indicated that P_x* was proportional to $D_f^{-1.53}$ (r^2 = 0.89). This was not consistent with kL being a constant, which requires that P_x* is

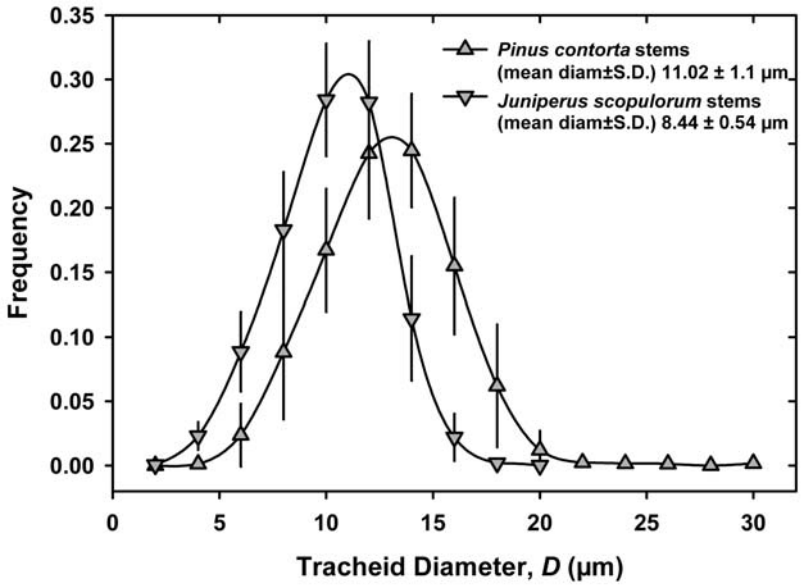

Figure 3. Tracheid diameter frequency distributions measured in *P. contorta* and *J. scopulorum* stem wood (n = 5–6; mean ± SD; SD bars may be smaller than symbols).

proportional to $D_f^{-2/3}$ (Fig. 4, dashed line). Nor was it consistent with $L \alpha D_f$, which predicts that P_x* should be proportional to D_f^{-1} (Fig. 4, dotted line). The kL declined with increasingly negative P_x* from an average of 1.45×10^{-4} μm at a P_x of -0.5 MPa to 9.35×10^{-7} μm at -8 MPa, and a one-way ANOVA revealed significant differences between the kL means (InStat; Fig. 5). These results indicate that the kL decreased systematically with more negative P_x*. Across the data set, P_x* was proportional to $(kL)^{-0.5}$ (Fig. 5; $r^2 = 0.96$).

DISCUSSION

The vulnerability of conifers to freeze-thaw embolism increases with greater tracheid diameter, and with increasingly negative P_x (Sperry and Sullivan, 1992; Davis et al., 1999; Feild and Brodribb, 2001; Mayr et al., 2002, 2003a, 2003b; Pittermann and Sperry, 2003; Stuart et al., 2005). In this study *J. scopulorum* was more resistant to freezing-induced embolism than *P. contorta* at a broad range of P_x, which is consistent with *J. scopulorum*'s narrower tracheid diameters (Figs. 2 and 3). As predicted, the PLC_{FT} in both species increased at more negative P_x (Fig. 2), consistent with an increasingly narrow threshold diameter from freeze-thaw-induced embolism (Fig. 4; Eq. 3). This implies that despite their inherent hydraulic inefficiency, the contribution of the narrower, more freeze-thaw-resistant tracheids is crucial in maintaining a fraction of hydraulic conductivity following a freeze-thaw cycle at more negative P_x. Assuming no

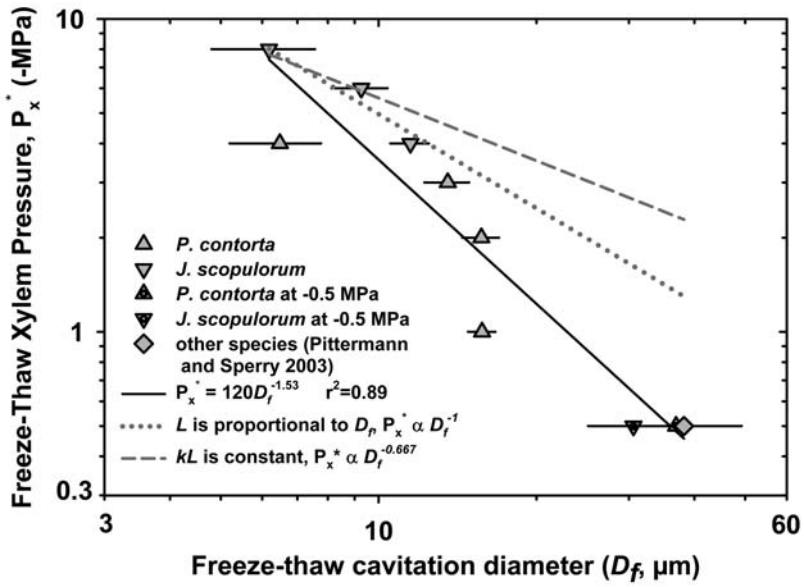

Figure 4. The relationship between the critical diameter (D_f) and the freeze-thaw xylem pressure, P_x* (n = 5–6; mean ± SD). The P_x* is plotted as the dependent variable for comparison with scaling predicted from Equation 3.

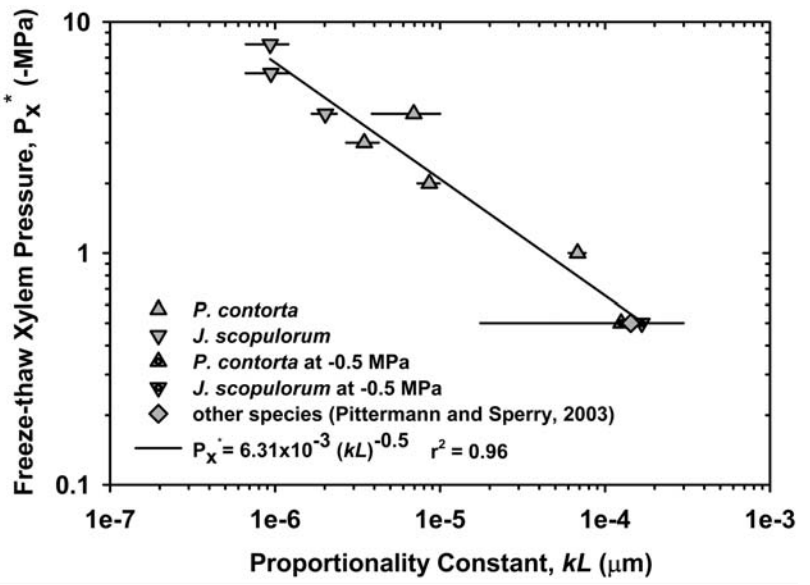

Figure 5. The *kL* coefficient plotted as a function of P_x^* (n = 5–6; mean ± SD). The P_x^* is plotted as the dependent variable for comparison with scaling predicted from Equation 3.

rapid reversal of embolism, this ''safety'' feature of tracheid-based wood is likely to be essential to the conifers' ability to quickly resume some degree of water transport following a freeze-thaw event, particularly when the tree is also water stressed (Sperry and Robson, 2001; Mayr et al., 2002, 2003a). By contrast, species bearing large-diameter conduits, such Quercus and Betula, have comparatively fewer narrow vessels and thus exhibit steep vulnerability curves that reach 100% PLC_{FT} at relatively mild xylem pressures (Sperry and Sullivan, 1992; Davis et al., 1999).

The decrease in critical diameter (D_f) with P_x^* is consistent with Equation 1, which predicts that smaller bubbles will nucleate embolism at more negative P_x^*. However, the observed scaling of $P_x^* \alpha D_f^{-3/2}$ (Fig. 4) indicated that *kL* was not constant but declined with P_x^* (Fig. 5). This decrease in *kL* has the additional effect of amplifying the gain in safety from freeze-thaw cavitation that comes from the narrowing of the conduit. The observed scaling indicates that a 10% narrowing in diameter achieves on average a 17% gain in negative P_x^* as opposed to only a 7% gain if *kL* were constant (Fig. 4, compare solid versus dashed lines).

Why should *kL* decline? A simple explanation is that *L*, the conduit length per bubble, declines in proportion with D_f, in which case Equation 3 predicts $P_x^* \alpha D_f^{-1}$. This could account for part of the *kL* decline but not all of it (Fig. 4, dotted line). The *k* term for proportionality between air and water volume may also decline with smaller D_f. Factors influencing *k* include the solubility of air in water, freezing rate, and bubble shrinkage as air dissolves back into the degassed sap during thawing when P_x is less than P_x^* (Robson et al., 1988; Robson and Petty, 1993; Langan et al., 1997; Sperry and Robson, 2001). The solubility of air in water and the freezing rate were unlikely to vary under the controlled conditions of the experiment or in any case to vary systematically with D_f. However, there is reason to suspect that smaller bubbles will shrink faster in diameter during thawing than bigger ones. According to the bubble dissolution model of Yang and Tyree (1992), the rate of dissolving increases with bubble pressure because of greater diffusion gradients in the liquid phase. The bubble pressure at $P_x = 0$ MPa should be inversely proportional to the bubble diameter according to the La Place equation (bubble pressure $= 4T/D_b$). Therefore, smaller bubbles will have greater gas pressure, causing them to dissolve faster than larger bubbles and shrink relatively more in diameter for the same thawing period before P_x drops to P_x^*. This would cause *k* to decrease with D_f, contributing to the $P_x^* \alpha D_f^{-3/2}$ scaling we observed (Fig. 4).

Bubble shrinkage is an important factor in vulnerability to freeze-thaw-induced cavitation. Observations of either frozen tracheids or comparably sized capillary tubes revealed bubbles whose diameters were estimated at 1 to 2 μm (Lybeck, 1959; Sucoff, 1969; Ewers, 1985; Robson et al., 1988; for angiosperms, see Utsumi et al., 1999). By contrast, we calculated that the largest possible bubble from our dataset based on a *kL* of 1.45×10^{-4} μm and D_f of 44 μm at -0.5 MPa would measure about 0.8 μm in diameter. This is less than one-half of the size of the bubbles observed by Sucoff (1969) and Robson et al. (1988) in frozen tracheids. The discrepancy is very likely a result of shrinkage during thaw. Negative pressure is eliminated by ice formation and it only returns after thawing has restored a continuous liquid water column (Hammel, 1967; Robson and Petty, 1987). In the interval between initial melting and the reappearance of negative pressure, the air bubbles have an opportunity to dissolve. The rate of dissolution is theoretically very rapid—a 2 μm bubble can dissolve in 0.1 s (Sucoff,

1969). The rapidity is in part owing to the strong diffusion gradient created by the degassed sap.

We might expect the centrifuge method to overestimate freezing-induced embolism because it minimizes the time required for the re-establishment of negative pressure after thawing. The stem is constantly spinning during the thaw, so negative pressure is restored at the instant the melt-water forms a liquid continuum across the stem. Bubbles might have less time to shrink and would be more likely to expand and nucleate cavitation. However, our *J. scopulorum* freeze-thaw vulnerability curve was similar to the *J. scopulorum* curve generated in a previous study where stems were progressively dehydrated, subjected to −20°C overnight in a freezer, and subsequently thawed over a 90-min period (Sperry and Sullivan, 1992). Similarly, Davis et al. (1999) found that centrifuge curves obtained for both gymnosperms and angiosperms were similar to freeze-thaw curves generated for the same species by the noncentrifuging method of Sperry and Sullivan (1992) as described above. The agreement between methods suggests that the bubbles have a similar time to dissolve regardless of how the negative pressure is established.

The results make it possible to roughly estimate the freeze-thaw + water-stress vulnerability curve of any conifer species from its tracheid diameter distribution. Using the empirical relationship between D_f and P_x* (Fig. 4):

$$P_x^* = 120 D_f^{-1.53}, \quad (4)$$

one can estimate D_f for any P_x* (P_x* in MPa, D_f in μm). From the diameter distribution, the loss of conductivity corresponding to tracheids larger than D_f can be calculated by assuming a proportionality between conductivity and the fourth power of the tracheid diameter. The modeled curves for the study species *P. contorta* and *J. scopulorum* (Fig. 6) do not correspond exactly with the experimental curves (Fig. 2) because they are based on the average scaling from the pooled data set. Furthermore, this analysis assumes that a tracheid of any given diameter will exhibit a particular freeze-thaw cavitation pressure at which it will unequivocally embolize due to freezing and thawing. This assumption may not be strictly true in vivo because the mechanism of freeze-thaw cavitation may involve a certain degree of stochasticity that could be due to some variation in bubble size, causing some tracheids to embolize while leaving others of equal diameter functional. However, the curves do reflect the relative differences in vulnerability. The estimated freeze-thaw + water-stress vulnerability curve of bald cypress (*Taxodium distichum*) stems is shown for comparison (Fig. 6) to illustrate the potential range of susceptibility to freezing-induced cavitation in conifers. Bald cypress has relatively large tracheids (mean diameter 40 ± 2.7 μm) and should be among the most vulnerable of conifers, whereas the Juniperus species have quite narrow tracheids and should be among the most resistant. Whether the putative vulnerability of Taxodium is a factor in its generally southern distribution and deciduous habit is unknown. Importantly, freeze-thaw + water-stress curves predicted from Equation 4 are only realistic if they are more vulnerable than the water-stress vulnerability curves; otherwise, the xylem is already cavitated by water stress. The predicted freezing curve for bald cypress does show greater vulnerability to freeze-thaw than to water stress alone, with the P_{50} of the freeze thaw curve shifted by approximately 1.5 MPa (data not shown; J. Pittermann, unpublished data). Equation 4 might also apply to vessels of angiosperms since they behave similarly to tracheids at P_x = −0.5 MPa (Pittermann and Sperry, 2003), but this remains to be confirmed.

There are many variables that potentially complicate the P_x* and diameter dependency of the freeze-thaw response—no doubt contributing to the scatter in

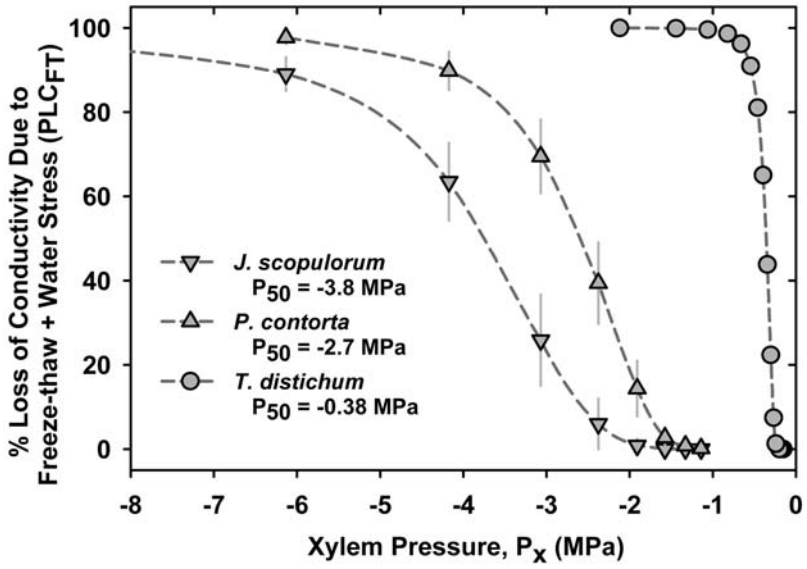

Figure 6. Freeze-thaw vulnerability curves estimated from tracheid diameter distributions and the P_x* versus D_f scaling in Figure 4. The means of n = 5 to 6 stem diameter distributions ± SD (subsample of distributions in Fig. 3) were used to construct the *P. contorta* and *J. scopulorum* curves. A curve for bald cypress (*T. distichum*) stems (mean tracheid diameter of 40 ± 2.7 μm) is shown for comparison.

the P_x* versus D_f scaling we observed (Fig. 4). Most fundamentally, our assumption that embolism will unequivocally occur in tracheids equal to or greater than a particular D_f is probably an oversimplification of a more stochastic relationship between bubble size, tracheid size, and vulnerability. However, dye perfusion experiments support a positive relationship between conduit diameter and vulnerability within single cross sections (Sperry and Sullivan, 1992). It is also plausible that in narrow and short tracheids, the average length (L) of the cylinder from which the bubble would normally be produced (Fig. 1) could become longer than the tracheid, in which case bubbles would be smaller than predicted. Although freezing and thawing rates and minimum temperature can influence freezing-induced cavitation (see below), these were controlled as much as possible in our experiments.

The freeze-thaw + water-stress and water-stress curves differed substantially from one another in both *J. scopulorum* and *P. contorta*, particularly at increasingly negative P_x (Fig. 2). Importantly, there is no obvious relationship between resistance to water stress and freeze-thaw embolism that would allow the response to one type of stress to be reliably predicted from the other. Whereas the basis for a relationship between tracheid diameter and freeze-thaw xylem pressure is straightforward and in principle independent of species (Sperry and Sullivan, 1992; Sperry et al., 1994; Hacke and Sauter, 1996; Davis et al., 1999; Cavender-Bares and Holbrook, 2001; Feild and Brodribb, 2001; Feild et al., 2002; Mayr et al., 2002; Pittermann and Sperry, 2003; Stuart et al., 2005), the structural basis for vulnerability to water stress is less apparent. Water-stress-induced cavitation is caused by air entry at the pit membrane (Sperry and Tyree, 1990; Hacke et al., 2004), but beyond this little is known of how pit and conduit structure causes cavitation resistance to vary (Wheeler et al., 2005).

Although freeze-thaw vulnerability curves are rarely presented, they are highly relevant to our understanding of the physiological ecology of temperate or tree-line conifers, because in mesic habitats conifers typically experience more embolism during the winter than during a summer drought (Sperry et al., 1994; Sparks and Black, 2000). Many agree that it is the combined stress of reduced water availability and freezing that produces winter embolism (Lemoine et al., 1999; Ameglio et al., 2001; Mayr et al., 2002, 2003a, 2003b), but the relative contribution of drought and freezing to winter embolism is unknown. Hence, carefully controlled freeze-thaw and water-stress experiments remain the most reliable method for teasing out species' responses to both types of stress.

The results presented in this study along with those of others have advanced our understanding of the mechanism of freeze-thaw embolism, yet a number of issues remain unclear. Variation in freezing and thawing rates could influence bubble sizes independent of tracheid diameter (Bari and Hallet, 1974; Robson and Petty, 1987; Robson et al., 1988; Sperry and Robson, 2001). It is known that faster thaw rates produce greater amounts of embolism, presumably because negative pressures are introduced into the xylem much quicker thereby favoring bubble expansion (Langan et al., 1997; Cordero and Nilsen, 2002). There is also an important effect of minimum temperature on PLC_{FT} in some material. *Larrea tridentata* stems and *Ginkgo biloba* roots showed an increase in embolism with cooler freezing temperature (Pockman and Sperry, 1997; Pittermann and Sperry, 2003; Cavender-Bares, 2005). In *L. tridentata*, the basis of this phenomenon has been tentatively attributed to freezing damage, which may weaken the resistance to water-stress-induced cavitation (Martínez-Vilalta and Pockman, 2002). Interestingly, the minimum temperatures required to eliminate conductivity in *L. tridentata* (−16°C to −20°C) corresponded to the distribution limits of this species in the Chihuahuan, Sonoran, and Mojave deserts (Pockman and Sperry, 1997; Martínez-Vilalta and Pockman, 2002).

CONCLUSION

Our work on the freeze-thaw response of *P. contorta* and *J. scopulorum* highlights the differences between water-stress and freeze-thaw + water-stress vulnerability curves and quantifies a reduction in D_f with increasingly negative P_x. We have refined our estimates of D_f by measuring the freeze-thaw response across a wide range of P_x from −0.5 MPa down to −8 MPa. The proportionality between P_x and D_f suggested that bubbles nucleating cavitation were smaller in proportion to tracheid diameter in narrower tracheids than in wider ones. This resulted in a 17% gain in safety (in P_x* terms) for a 10% narrowing of diameter. The amplified safety of narrow conduits may result from faster shrinkage of smaller bubbles during thaw than larger bubbles. The empirical relationship between D_f and P_x* allowed us to roughly predict the conifer freeze-thaw response, and might apply to angiosperms as well. More observations of bubble size distributions in conduits or in capillary tube analogs (Ewers, 1985; Robson et al., 1988) and size distributions of embolized versus nonembolized conduits (Utsumi et al., 1998, 1999, 2003) would improve our understanding of the link between diameter and vulnerability.

MATERIALS AND METHODS

Plant Material

Stem samples of *Pinus contorta* Dougl. ex Loudon (Pinaceae) and *Juniperus scopulorum* (Cupressaceae) were collected in the Uinta/Wasatch-Cache National Forest in northern Utah (40°3′ N, 111°47′ W) in October 2003. *J. scopulorum* is significantly more resistant to air-seeding and freeze-thaw embolism than *P. contorta*, and these two species represent much of the broad range in tracheid diameters and drought/freeze-thaw embolism responses found in nature (Hacke et al., 2001; Pittermann and Sperry, 2003). Stems

varying from 8 to 10 mm in diameter were cut from adult trees, wrapped in damp paper towels, double-bagged to prevent water stress, and transported to the laboratory. The selected stems were straight, no less than 20 cm in length, and cut from healthy trees growing in moist soils. The freeze-thaw experiments described below were completed within 4 d of collecting the plant material.

Hydraulic Conductivity Measurements

The hydraulic conductivity (volume flow rate/pressure gradient; K) was measured in the laboratory, as described by Pittermann and Sperry (2003). Wood samples were recut under water to a length of 142 mm, and the distal ends shaved smooth with a razor blade. The bark was left intact on the stem segments with the exception of the distal ends, where 1 cm of bark was removed to avoid clogging with resin. The K was measured gravimetrically with a pressure head of 4 to 5 kPa, using distilled and filtered (0.22 μm) water.

Vulnerability Curves

Three K measurements were made per stem to assess the effect of water stress and freeze-thaw cycles + water stress on embolism. We initially measured the stem's native conductivity (K_{native}). We did not flush the stems to remove native emboli because in preliminary measurements the conductivity consistently decreased slightly following the flush, meaning there was no detectable native embolism. Next, the stem was spun in a custom centrifuge rotor for 3 min at 20°C to induce a known P_x (Alder et al., 1997). The rotor can hold up to three segments, and was designed for a Sorvall RC5C centrifuge. The K was remeasured to assess the effect of P_x on the conductivity (K_{ws}), and the percentage of loss of K due to water stress (PLC_{ws}) was calculated according to $PLC_{ws} = 100 \times (1 - (K_{ws}/K_{native}))$. The same stem was returned to the centrifuge, spun at the same P_x as before while being frozen and thawed. The K was measured a third time to determine the additional effect of the freeze-thaw treatment (K_{FT}). The PLC after freezing and thawing (PLC_{FT}) was related to K_{native}, such that $PLC_{FT} = 100 \times (1 - (K_{FT}/K_{native}))$.

The temperature during the freeze-thaw cycle was controlled by the centrifuge refrigeration settings and by an external bath (model 1157; VWR Scientific) that circulated heat transfer fluid (type XLT; Polyscience) through copper tubing lining the rotor chamber. The centrifuge and the bath were set to −3°C and −20°C, respectively, at the start of the freeze-thaw experiment. The low bath temperature compensated for the weak cooling capacity of the centrifuge and thus helped to chill the rotor. Once the segments reached the desired P_x, centrifuge temperatures were reduced by 3°C every 18 min to a minimum of −15°C for the first 90 min of the freezing treatment. The cooling rate was approximately 0.2°C min^{-1}, such that the minimum temperatures of the segments reached −8°C to −14°C (Pittermann and Sperry, 2003). Subsequently, the stems were thawed during the remaining 90 min of centrifugation, also at a rate of about 0.2°C min^{-1}. After this 3-h freeze-thaw cycle, the K was measured to determine the effect on conductivity (K_{FT}) as explained in the previous paragraph.

Control experiments showed that the 3-h centrifuge treatment without the intervening freeze-thaw cycle had no effect on stem conductivity (Pittermann and Sperry, 2003).

In *P. contorta*, the K_{WS} and K_{FT} data were obtained at P_x ranging from −1 to −4 MPa in 1 MPa increments, where freezing-induced embolism reached values greater than 90% at −4 MPa. The range of P_x was much broader for *J. scopulorum*: PLC values were measured in 2 MPa increments and reached 90% at −8 MPa. Between five and six stems were tested at each P_x in both the water-stress and freeze-thaw treatments.

Tracheid Diameter Measurements

Anatomical measurements were obtained from the stem material used in the freeze-thaw experiments described above. Hand-cut, transverse sections were cut from the center of the stem, stained in Toluidine Blue, rinsed in distilled water, and mounted in glycerin. The sections were viewed and photographed at 400× with a Nikon Eclipse E600 microscope and digital camera (model RT KE; Diagnostic Instruments). Tracheid areas were measured using image analysis software (Image-Pro; Media Cybernetics) and then converted to equivalent circle diameters. Three to four radial files of tracheids were measured within a minimum of four growth rings in at least three different sectors of the cross section. This gave a total of no less than 600 tracheid diameters per stem.

Estimation of D_f and kL

If Equation 4 correctly describes the freeze-thaw response, and bubble size increases with tracheid diameter, there will be a D_f above which tracheids will embolize due to freezing at a given P_x. We calculated the D_f for each of the stems tested across the range of P_x from the stems' tracheid diameter (D) distribution. We assumed that tracheid conductivity is proportional to the fourth power, consistent with the Hagen-Poiseuille equation. Although tracheid conductivity is less than the Hagen-Poiseuille values, recent results indicated it falls short by a similar fraction across species (Sperry et al., 2005). The cumulative D^4 distribution for a stem thus represents the increase in relative conductivity of the stems tracheids from small to large. By fitting the cumulative D^4 distribution with a Weibull function, we could calculate the D_f from the inverse of the function and the PLC_{FT}:

$$D_f = b(-\ln(PLC_{FT}/100))^{(1/c)}, \quad (5)$$

where b and c are the Weibull function coefficients. When the mean PLC_{FT} of the pooled stems was significantly greater than the mean PLC_{WS} for a specific P_x (i.e. freezing and thawing + water stress caused more embolism than water stress alone; Student's t test at 5% significance level, n = 5–6), we used Equation 5 to solve for D_f for each individual stem from its PLC_{FT} and tracheid diameter distribution.

This analysis assumes that the largest-diameter tracheids are not only the most vulnerable to freeze-thaw embolism as expected from theory, but also that they are most vulnerable to the initial water-stress treatment. This assumption is consistent with dye perfusion experiments on several conifer species, such as *Juniperus virginiana*, *Picea rubra*, and *Abies balsamea* (Sperry and Tyree, 1990; see also Cochard, 1992), which showed that earlywood tracheids embolize at less negative P_x than latewood. Although latewood in Douglas fir *(Pseudotsuga menziesii)* can begin to embolize before earlywood, even in this species much of the latewood remains more resistant than the earlywood at more negative P_x (Domec and Gartner, 2002).

Last, we calculated the kL from each stem's D_f by solving Equation 3 for kL.

Analysis of Data from Pittermann and Sperry (2003)

The D_f values for species analyzed at −0.5 MPa from Pittermann and Sperry (2003) were originally calculated by assuming $PLC_{WS} = 0$, meaning that any embolism that occurred was assumed to be from freezing and thawing. Although this was approximately the case for this mild pressure (see also Davis et al., 1999), for the sake of consistency and greater precision in the D_f and kL estimates, we reanalyzed these results as described above. The data from Pittermann and Sperry (2003) were from the roots and stems of *J. scopulorum*, *P. contorta*, and bald cypress (*Taxodium distichum*), the roots of *Abies concolor* and *Abies lasiocarpa*, and the stems of *Gingko biloba.*

Received June 30, 2005; revised September 27, 2005; accepted October 26, 2005; published December 23, 2005.

LITERATURE CITED

Alder NN, Pockman WT, Sperry JS, Nuismer S (1997) Use of centrifugal force in the study of xylem cavitation. J Exp Bot **48:** 665–674

Ameglio T, Ewers FW, Cochard H, Martignac M, Vandame M, Bodet C, Cruiziat P (2001) Winter stem xylem pressure in walnut trees: effects of carbohydrates, cooling and freezing. Tree Physiol **21:** 387–394

Bari SA, Hallet J (1974) Nucleation and growth of bubbles at an ice/water interface. J Glaciology **8:** 489–529

Cavender-Bares J (2005) Impacts of freezing on long-distance transport in woody plants. *In* NM Holbrook, MA Zwieniecki, eds, Vascular Transport in Plants. Elsevier Academic Press, San Diego, pp 401–424

Cavender-Bares J, Holbrook NM (2001) Hydraulic properties and freezing-induced cavitation in sympatric evergreen and deciduous oaks with contrasting habitats. Plant Cell Environ **24:** 1243–1256

Cochard H (1992) Vulnerability of several conifers to air embolism. Tree Physiol **11:** 73–83

Cordero RA, Nilsen ET (2002) Effects of summer drought and winter freezing on stem hydraulic conductivity of Rhododendron species from contrasting climates. Tree Physiol **22:** 919–928

Davis SD, Sperry JS, Hacke UG (1999) The relationship between xylem conduit diameter and cavitation caused by freezing. Am J Bot **86:** 1367–1372

Domec J-C, Gartner BL (2002) How do water transport and water storage differ in coniferous earlywood and latewood? J Exp Bot **53:** 2369–2379

Ewers FW (1985) Xylem structure and water conduction in conifer trees, dicot trees, and lianas. Int Assoc Wood Anat Bull **6:** 309–317

Feild TS, Brodribb T, Holbrook NM (2002) Hardly a relict: freezing and the evolution of vesselless wood in Winteraceae. Evolution Int J Org Evolution **56:** 464–478

Feild TS, Brodribb TJ (2001) Stem water transport and freeze-thaw embolism in conifers and angiosperms in a Tasmanian treeline heath. Oecologia **127:** 314–320

Hacke U, Sauter JJ (1996) Xylem dysfunction during winter and recovery of hydraulic conductivity in diffuse-porous and ring-porous trees. Oecologia **105:** 435–439

Hacke UG, Sperry JS, Pittermann J (2004) Analysis of circular bordered pit function II. Gymnosperm tracheids with torus-margo pit membranes. Am J Bot **91:** 386–400

Hacke UG, Sperry JS, Pockman WP, Davis SD, McCulloh KA (2001) Trends in wood density and structure are linked to prevention of xylem implosion by negative pressure. Oecologia **126:** 457–461

Hammel HT (1967) Freezing of xylem sap without cavitation. Plant Physiol **42:** 55–66

Langan S, Ewers FW, Davis SD (1997) Xylem dysfunction caused by water stress and freezing in two species of co-occurring chaparral shrubs. Plant Cell Environ **20:** 425–437

Lemoine D, Granier A, Cochard H (1999) Mechanism of freeze-induced embolism in *Fagus sylvatica* L. Trees **13:** 206–210

Lybeck BR (1959) Winter freezing in relation to the rise of sap in tall trees. Plant Physiol **34:** 482–486

Martínez-Vilalta J, Pockman WT (2002) The vulnerability to freezing-induced xylem cavitation of *Larrea tridentata* (Zygophyllaceae) in the Chihuahuan desert. Am J Bot **89:** 1916–1924

Mayr S, Gruber A, Bauer H (2003a) Repeated freeze-thaw cycles induce embolism in drought stressed conifers (Norway spruce, stone pine). Planta **217:** 436–441

Mayr S, Schwienbacher F, Bauer H (2003b) Winter at the Alpine timberline. Why does embolism occur in Norway spruce but not in stone pine? Plant Physiol **131:** 780–792

Mayr S, Wolfschwenger M, Bauer H (2002) Winter-drought induced embolism in Norway spruce (*Picea abies*) at the Alpine timberline. Physiol Plant **115:** 74–80

Pittermann J, Sperry JS (2003) Tracheid diameter is the key trait determining the extent of freezing-induced cavitation in conifers. Tree Physiol **23:** 907–914

Pockman WT, Sperry JS (1997) Freezing-induced xylem cavitation and the northern limit of Larrea tridentata. Oecologia **109:** 19–27

Pockman WT, Sperry JS, O'Leary JW (1995) Sustained and significant negative water pressure in xylem. Nature **378:** 715–716

Robson DJ, McHardy WJ, Petty JA (1988) Freezing in conifer xylem: pit aspiration and bubble formation. J Exp Bot **39:** 1617–1621

Robson DJ, Petty JA (1987) Freezing in conifer xylem: pressure changes and growth velocity of ice. J Exp Bot **38:** 1901–1908

Robson DJ, Petty JA (1993) A proposed mechanism of freezing and thawing in conifer xylem. *In* M Borghetti, J Grace, A Raschi, eds, Water Transport in Plants under Climatic Stress. Cambridge University Press, Cambridge, UK, pp 75–85

Scholander PF, Hemmingsen EA, Garey W (1961) Cohesive lift of sap in the Rattan vine. Science **134:** 1835–1838

Sparks JP, Black RA (2000) Winter hydraulic conductivity and xylem cavitation in coniferous trees from upper and lower treeline. Arct Antarct Alp Res **32:** 397–403

Sparks JP, Campbell GS, Black RA (2001) Water content, hydraulic conductivity, and ice formation in winter stems of *Pinus contorta*: a TDR case study. Oecologia **127:** 468–475

Sperry JS, Hacke UG, Wheeler JW (2005) Comparative analysis of end wall resistance in xylem conduits. Plant Cell Environ **28:** 456–465

Sperry JS, Nichols KL, Sullivan JEM, Eastlack SE (1994) Xylem embolism in ring-porous, diffuse-porous, and coniferous trees of northern Utah and interior Alaska. Ecology **75:** 1736–1752

Sperry JS, Robson DJ (2001) Xylem cavitation and freezing in conifers. *In* FJ Bigras, SJ Colombo, eds, Conifer Cold Hardiness. Kluwer Academic Publishers, Dordrecht, The Netherlands, pp 121–136

Sperry JS, Sullivan JEM (1992) Xylem embolism in response to freeze-thaw cycles and water stress in ring-porous, diffuse-porous, and conifer species. Plant Physiol **100:** 605–613

Sperry JS, Tyree MT (1990) Water-stress-induced xylem embolism in three species of conifers. Plant Cell Environ **13:** 427–436

Stuart SA, Choat B, Holbrook NM, Ball MC (2005) How freezing sets the latitudinal limit of mangrove forests. Honors thesis, Harvard University, Cambridge, MA

Sucoff E (1969) Freezing of conifer xylem and the cohesion tension theory. Physiol Plant **22:** 424–431

Utsumi Y, Sano Y, Fujikawa S, Funada R, Ohtani J (1998) Visualization of cavitated vessels in winter and refilled vessels in spring in diffuse-porous trees by cryo-scanning electron microscopy. Plant Physiol **117:** 1463–1471

Utsumi Y, Sano Y, Funada R, Fujikawa S, Ohtani J (1999) The progression of cavitation in earlywood vessels of *Fraxinus mandshurica* var *japonica* during freezing and thawing. Plant Physiol **121:** 897–904

Utsumi Y, Sano Y, Funada R, Ohtani J, Fujikawa S (2003) Seasonal and perennial changes in the distribution of water in the sapwood of conifers in a sub-frigid zone. Plant Physiol **131:** 1826–1833

Wheeler JK, Sperry JS, Hacke UG, Hoang N (2005) Inter-vessel pitting and cavitation in woody Rosaceae and other vesselled plants: a basis for a safety versus efficiency trade-off in xylem transport. Plant Cell Environ **28:** 800–812

Yang S, Tyree MT (1992) A theoretical model of hydraulic conductivity recovery from embolism with comparison to experimental data on *Acer saccharum.* Plant Cell Environ **15:** 633–643

Zimmermann MH (1983) Xylem Structure and the Ascent of Sap. Springer-Verlag, Berlin